교육학 석사학위논문

Fabrication of Multiwalled carbon nanotube-Polydopamine-Prussian blue nanocomposites and its application for hydrogen peroxide sensing

탄소나노튜브-폴리도파민-프러시안 블루
나노복합물의 합성과 과산화수소의 검출 연구

2015년 2월

서울대학교 대학원
과학교육과 화학전공
권 정 희

Fabrication of Multiwalled carbon nanotube -Polydopamine-Prussian blue nanocomposites and its application for hydrogen peroxide sensing

탄소나노튜브-폴리도파민-프러시안 블루 나노복합물의 합성과 과산화수소의 검출 연구

지도교수 홍 훈 기

이 논문을 교육학 석사학위논문으로 제출함

2014년 12월

서울대학교 대학원

과학교육과 화학전공

권 정 희

권정희의 석사학위논문을 인준함

2014년 12월

위 원 장 _____ (인)

부 위 원 장 _____ (인)

위 원 _____ (인)

CONTENT

List of Table

List of Figures

Abstract

Fabrication of Multiwalled carbon nanotube-Polydopamine-Prussian blue nanocomposites and its application for hydrogen peroxide sensing

Joung-Hee Kwon
Chemistry Education Major
Department of Science Education
The Graduate School
Seoul National University

In this study, we presented a simple method for the synthesis of multiwalled carbon nanotube-polydopamine-prussian blue (MWCNT-PDA -PB) nanocomposites. MWCNTs were easily coated with PDA at room temperature. MWCNT-PDA-PB nanocomposites could be synthesized by adding the MWCNT-PDA to an acidic solution of Fe^{3+}, $Fe(CN)_6^{3-}$ and

KCl. The PDA layer not only improved dispersion of MWCNTs in water, but also assisted the formation and immobilization of PB NPs on the surface of MWCNTs. The morphology and chemical composition of the MWCNT-PDA-PB nanocomposites were characterized by Transmission electron microscopy (TEM), Fourier transform infrared spectroscopy (FT-IR), and X-ray diffraction (XRD).

The electrochemical behavior of the MWCNT-PDA-PB modified electrode was investigated using cyclic voltammetry and amperometry. The modified sensor showed a good electrocatalytic response toward the reduction of hydrogen peroxide. The sensor exhibited a linear response for H_2O_2 over concentrations ranging from 0.001–1.84 mM with a high sensitivity of 351.2 μA $mM^{-1}cm^{-2}$ and a low detection limit (S/N=3) of 0.039 μM. These parameters compare favorably with other CNT-PB based electrodes. This work describes a new type of PDA-carbon material-modified electrode for biosensors.

Key words: Multi-walled carbon nanotubes (MWCNTs), Polydopamine (PDA), Prussian blue (PB), Hydrogen peroxide (H_2O_2), Amperometry.

Student Number **: 2013-21424**

Fabrication of Multiwalled carbon nanotube-Polydopamine-Prussian blue nanocomposites and its application for hydrogen peroxide sensing

1. Introduction

Carbon nanotubes (CNTs) have attracted scientific interest as the materials of future nanotechnology for their unique electronic properties, high chemical stability, and mechanical strength [1,2]. CNTs' poor solubility in water and tendency to aggregate, however, require surface modification for the successful application of CNT-based composite materials [3–5]. A wide variety of modifications have been used to improve the handling of CNTs [6]. One of the most widely-used approaches is the covalent functionalization of CNTs which employs covalent attachment of chemical groups such as oxidation and fluorination under high temperatures or/and pressures [7–9]. Although covalent modification is broadly utilized, covalent modification has the drawback of damaging the physical properties of the CNTs [10]. Meanwhile, non-covalent functionalization of CNTs is also attractive in that it can combine chemical moieties without affecting the electrical structure of the nanotubes [6]. The non-covalent approach, based on van der Waals forces or π–π stacking interactions, mainly includes polymer adsorption and wrapping [11–13]. A vast array of methods using various polymers has been suggested.

Lee et al. has recently proposed a unique approach to surface modification by polydopamine (PDA) using dopamine (DA) self-polymerization inspired by mussel adhesion protein [14]. This environmentally friendly process occurs simply by immersing the substrate in a dopamine alkaline solution at room temperature. As an organic semiconductor of melanin-like structure, PDA has multifunctional groups (amino and catechol groups) and is hydrophilic

and biocompatible. PDA can be used as an ad-layer onto a wide range of surfaces, including noble metals, oxides, polymers, semiconductors, and ceramics [14]. Moreover, PDA coatings can serve as a versatile platform for secondary surface-mediated reactions, leading to tailoring of the coatings for diverse functional uses. For example, PDA can deposit adherent and uniform metal coating onto substrate by electroless metallization [15–17]. Where the apparent reductive capacity of the PDA sublayer eliminates the need for addition of hazardous reducing agents such as hydrazine or $NaBH_4$. For these fascinating properties (reduction and adhesion), PDA has been widely used in biosensing applications [17–20].

Hydrogen peroxide (H_2O_2) is a dangerous chemical substance to the environment and a byproduct of industry and nuclear plants [21,22]. It is also a byproduct of enzymatic reactions and is known as one of the risk factors in the progression of major human diseases [21,22]. Therefore, a more reliable, accurate, sensitive and low-cost detection of H_2O_2 has become extremely important in recent years. Prussian Blue (PB) is the prototype of polynuclear transition-metal hexacyanometalates. PB has received much attention of the biosensor community for its ability to reduce hydrogen peroxide. Due to the high selectivity for the reduction of oxygen and hydrogen peroxide, PB is often considered as an “artificial peroxidase enzyme” [23]. The traditional synthesis of PB is based on a direct precipitation reaction of the Fe^{m+} cations and the $[Fe(CN)_6]^{n-}$ anions in a neutral aqueous solution [24]. This rapid reaction process, however, makes it difficult to control over the size and morphology of the products [24]. Meanwhile, it has been reported that PB nanomaterials could also be prepared by directly mixing Fe^{3+} and $Fe(CN)_6^{3-}$ in the presence of reducing agents such as single-walled

carbon nanotubes (SWNTs) [25], graphene [26], and MWCNTs [27,28]. With this slow reaction process, it has been possible to control the properties of PB NPs such as particle size distribution and particle shape [24].

In this work, MWCNTs were functionalized with self-polymerized PDA layer, followed by the decoration with PB NPs by chemical deposition. The MWCNT-PDA composites were prepared by simply dispersing MWCNTs in DA aqueous solution. In acidic media, electroless PB deposition was achieved on PDA coated MWCNT by mixing it with PB precursors ($K_3Fe(CN)_6$ and $FeCl_3$) for an hour. PDA was used as a polymer matrix to combine the good electronical conductivity of MWCNTs and the high electrocatalytic activity of PB toward H_2O_2. The multi-functionality of PDA adhesion layer made it easier to achieve the homogeneous formation and immobilization of the PB NPs. It was found that PDA modification not only improved the dispersion of MWCNTs in aqueous solution, but also aided the stability of the electrode due to PDA's adhesive property. Also, the MWCNT-PDA-PB composites could readily be produced without reducing agents or toxic solvents. The green method presented here demonstrates a promising MWCNT-PDA based composites synthesized with inorganic nanoparticles (NPs) for the construction of biosensors.

2. Experimental

2.1. Chemicals and reagents

Multi-walled carbon nanotubes (MWCNTs, 95% purity, diameter 10-15 nm, Iljin, Korea) were used without further purification. Dopamine hydrochloride, 2-amino-2-(hydroxymethyl)-1,3-propanediol (99.9%), acetic acid (99.0 wt% in H_2O), potassium ferricyanide(III) ($K_3Fe(CN)_6$, 99+%), Iron(III) chloride ($FeCl_3$, 97%), hydrogen peroxide (H_2O_2 , 30 wt% in H_2O), Nafion (~5% in a mixture of lower aliphatic alcohols and water), ascorbic acid, and uric acid were purchased from Sigma–Aldrich (USA). L-cysteine was purchased from Yakuri Pure Chemicals Co. (Japan). All other chemicals were of analytical grade and used without further purification. All solutions were prepared with deionized water obtained from an ultrapure water purification system (Human Co., Korea) with a resistivity of not less than 18.2 MΩ cm.

2.2. Apparatus and measurements

Cyclic voltammetry (CV) and amperometry were performed using a computer-controlled CHI 842 B potentiostat with a conventional three-electrode system. A glass carbon working electrode (3 mm diameter, GCE) was used in the preparation of the modified electrode. A platinum (Pt) counter electrode and a silver/silver chloride (Ag/AgCl,

3 M KCl) reference electrode were used to complete the three-electrode system. Transmission electron microscopy (TEM) measurements were performed on a LIBRA 120 with an accelerating voltage of 120 kV, and the samples for TEM were prepared by placing a drop of the dispersion on a carbon-coated copper grid. Fourier transform infrared spectra (FT-IR) were recorded with a Perkin-Elmer Spectrum 2000 FT-IR spectrometer in the range of 400 – 4000 cm^{-1} using a KBr pellet. X-ray diffraction (XRD) analyses were performed on a New D8 Advance diffractometer. All ultrasonic cleaning was done using a US-2510 Ultrasonic Cleaner (Branson, USA).

2.3. Fabrication of MWCNT-PDA nanocomposites

MWCNT-PDA nanocomposites were prepared as reported previously [29]. In brief, 0.05 mg mL^{-1} dopamine was prepared in 10 mM Tris (pH 8.5), and 20 mg MWCNT was well dispersed into 200 mL of the above solution by a 30-min sonication. After gently stirring for about 24 h, the coated MWCNT (MWCNT-PDA) were carefully filtered through a membrane filter (with a pore size of 0.2 μm), washed with deionized water several times and dried overnight in oven at 40 °C. The material was finally redispersed in acid solution at pH 6.5.

2.4. Preparation of MWCNT-PDA-PB nanocomposites

The above MWCNT-PDA nanocomposite dispersion (0.8 mL at a concentration of 0.5 mg mL^{-1}) was added into 25 mL of a 0.1 M KCl aqueous solution (pH 2.7, adjusted with acetic acid) containing 1 mM $K_3Fe(CN)_6$, under stirring for 5 min. 1 mM $FeCl_3$ was then added dropwise to this mixture with continuous stirring at room temperature. After 1 h, the obtained dispersion was filtered, centrifuged, washed with deionized water several times and finally redispersed in 10 mL of water.

2.5. Preparation of MWCNT-PDA-PB modified GCE

Prior to the modification, a glassy carbon electrode (GCE) was polished with 0.3, and 0.05 μm alumina slurry to produce a mirror-like surface. It was then rinsed thoroughly with deionized water and ultrasonicated in deionized water for 2 min. After the electrode was dried, 8 μL of the above MWCNT-PDA-PB dispersion was dropped onto the purified GC surface and dried in an oven at 40 °C for 2 h. Next, 2 μL of Nafion (0.5 wt % in water) was also placed on the surface and the system was then allowed to dry in an oven at 40 °C for an hour.

3. Results and Discussion

3.1. Characterization of the MWCNT-PDA and MWCNT-PDA-PB nanocomposites

The synthesis of the MWCNT-PDA PB nanocomposites is illustrated in Scheme 1. We prepared MWCNT-PDA-PB nanocomposites by two steps. First, MWCNTs were dispersed in a weak alkaline solution of DA and mildly stirred for 24 h to prepare MWCNT-PDA composites. And then, electroless PB deposition was achieved on MWCNT-PDA by simply mixing with PB precursors ($K_3Fe(CN)_6$ and $FeCl_3$) for an hour. The morphology and size of nanocomposites were characterized by TEM analysis (Fig. 1). MWCNTs in Fig. 1B are fatter than the pure MWCNTs (Fig. 1A), under the same magnification, implying that MWCNTs have been coated with PDA layer. In Fig. 1B, the interface between MWCNTs sidewall and PDA coating is observed, and the thickness of PDA films is about 2-3 nm. The insets of Fig. 1A and B are the digital photos of the materials in water (pH 6.5), which were kept still for 7 days after sonication. The solubility of MWCNTs was largely improved after being immersed in a dopamine (DA) solution, indicating that PDA was successfully grafted on the surface of MWCNTs. In acidic condition, protonated amine groups in PDA bring about the good solubility of MWCNT-PDA [30].

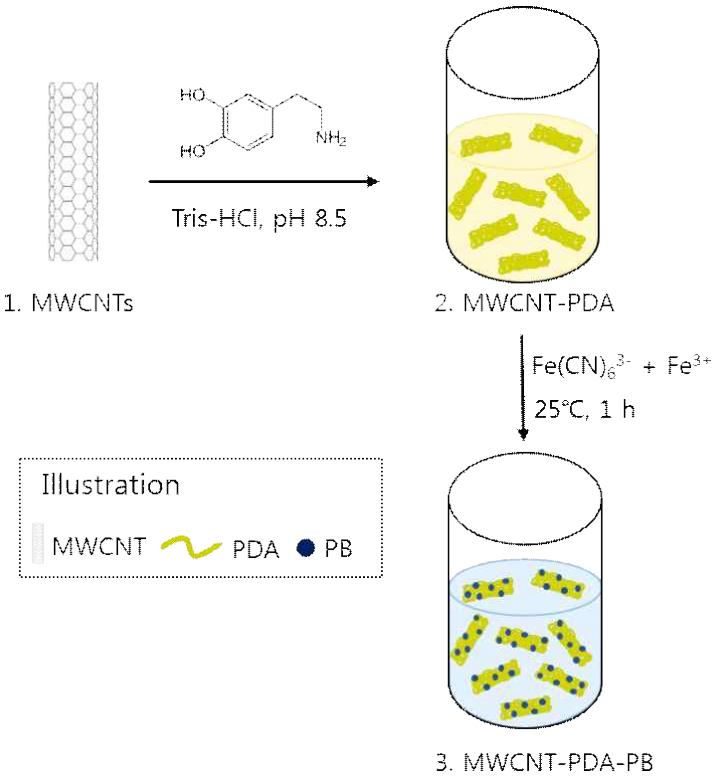

Scheme 1. Synthesis of MWCNT-PDA-PB nanocomposites.

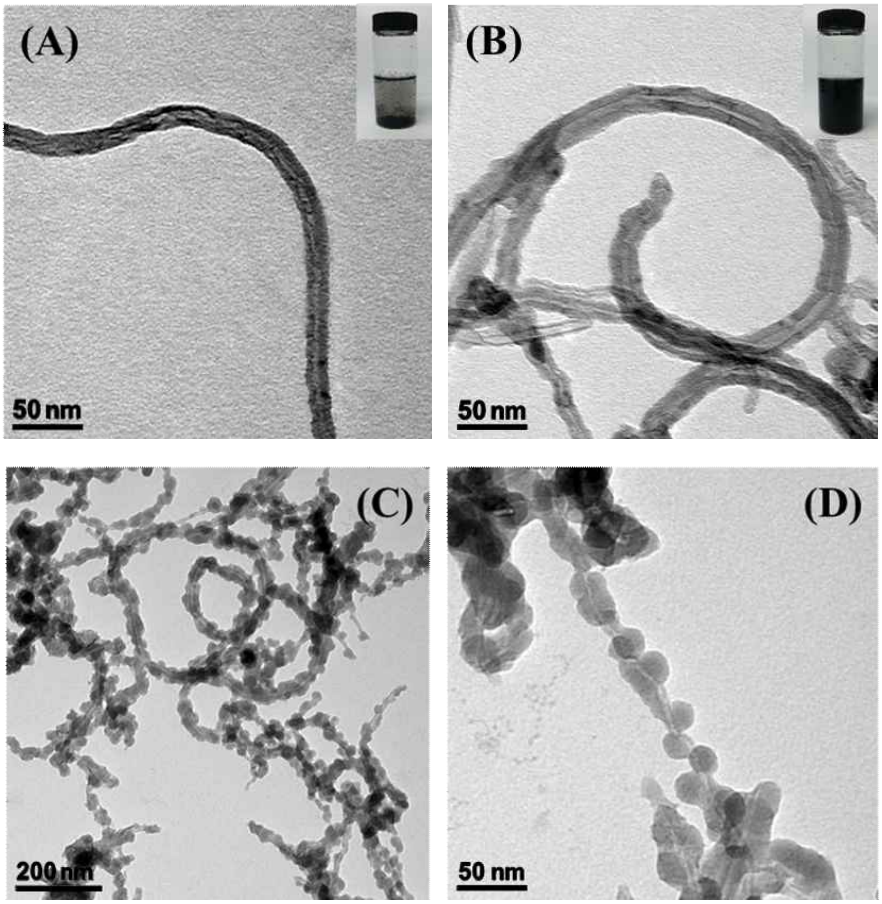

Figure 1. TEM images of MWCNTs (A), MWCNT-PDA (B), MWCNT-PDA-PB nanocomposites at different magnification (C and D). Inset A and B are the digital photos of the desired sample in water (pH 6.5).

In this work, we set DA concentration at 0.05 mg mL^{-1} in order to prevent generation of impurities. Because When concentration of DA above 0.1 mg mL^{-1} produced plenty of PDA precipitates which were not only hard to separate, but also hampered the modification of MWCNTs [30]. Figure 1C and D show PB NPs homogeneously decorated on the surface of MWCNT-PDA layer after treatment with the solution of Fe^{3+} and $Fe(CN)_6^{3-}$ for an hour. Thus, the TEM images demonstrate that this method can effectively generate PB NPs on the MWCNT hybrids.

The formation of MWCNT-PDA-PB nanocomposites was further characterized by FTIR. In Fig. 2A, MWCNT-PDA (Fig. 2A(b)) shows intense absorption peaks around 1640 cm^{-1} from aromatic rings and around 3440 cm^{-1} from catechol-OH groups, respectively, while MWCNT (Fig. 2A(a)) presents a weaker absorption band at the same position. These features support the coating of MWCNT by PDA [15,31]. Compared to the spectrum of MWCNT-PDA, MWCNT-PDA-PB nanocomposites show a strong absorption band around 2076 cm^{-1}, which is the common characteristics of C≡N stretching band in the $Fe^{2+}-CN-Fe^{3+}$ of PB. The absorption band at 499 cm^{-1} is due to the formation of M-CN-M' structure (M = metal). Both bands indicate the presence of PB [32].

The composition of the as-prepared nanocomposites was also examined by XRD measurement (Fig. 2B). The peaks at 2θ = 26.33° and 42.58° correspond to the (0 0 2) and (1 0 0) reflections of MWCNT's graphite-like structure, respectively [33]. The reflections of MWCNT-PDA (Fig. 2B(b)) are remarkably consistent with MWCNTs (Fig. 2B(a)), indicating that PDA coating doesn't destroy the crystal

structure of graphite from MWCNTs [33]. After the formation of PB NPs on the surface of MWCNT-PDA nanocomposites, the peaks were observed at 2θ = 17.5°, 24.8°, 35.4°, 39.8°, 50.9°, 54.3°, 57.5° which correspond to the (2 0 0), (2 2 0), (4 0 0), (4 2 0), (4 4 0), (6 0 0), and (6 2 0) reflections, respectively (Fig. 2B(c)). All of these reflections definitively demonstrated the successful synthesis of PB [34]. The mean diameter of PB NPs was calculated using the Scherrer formula [35]:

$$t = \frac{0.9\lambda}{B\cos\theta_B}$$

The linewidth B is usually measured at the half-maximum intensity from the strongest diffraction line (the (2 0 0) diffraction line). Where θ_B is the Bragg angle for the reflection, t the crystal size, and λ the wavelength of the X-ray. The calculated mean diameter of the PB NPs was approximately 12.8 nm, which was similar to the measured diameter of 13 nm. The latter is the average diameter of five randomly sampled NPs from the TEM image.

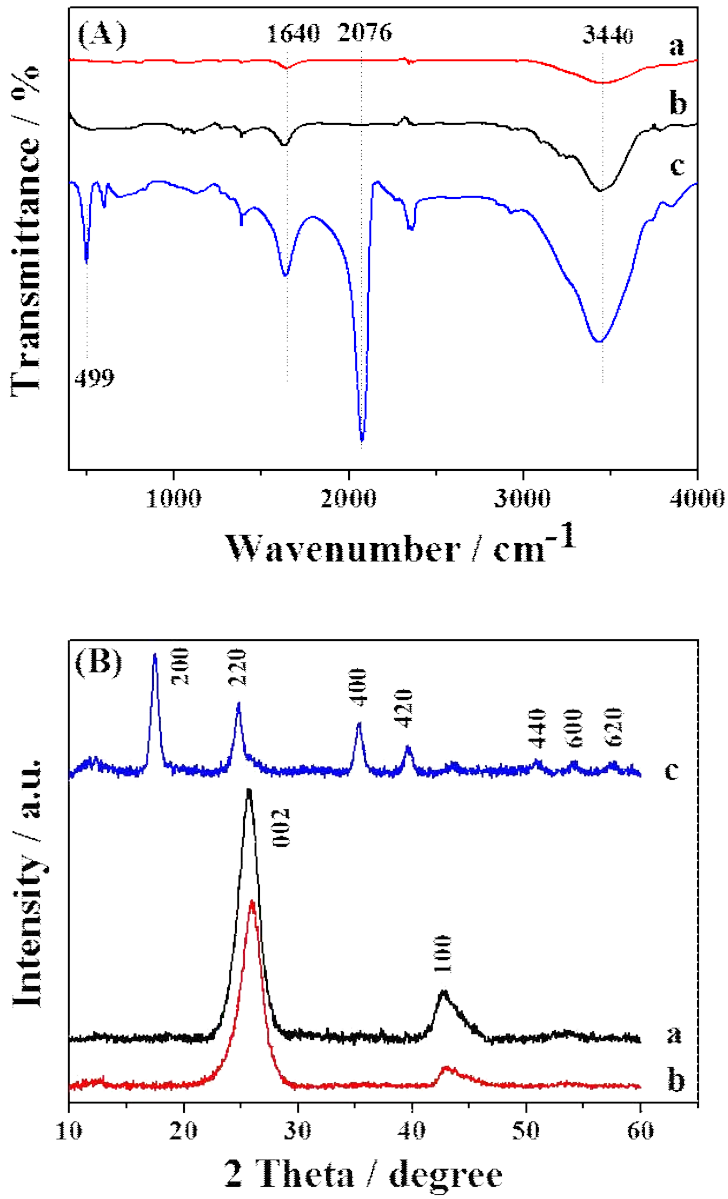

Figure 2. (A) FTIR spectra of (a) MWCNT, (b) MWCNT-PDA, (c) MWCNT-PDA-PB nanocomposites ; (B) XRD patterns of (a) MWCNT, (b) MWCNT-PDA (c) MWCNT-PDA-PB nanocomposites.

With the obtained results, a probable explanation for the formation mechanism of MWCNT-PDA-PB nanocomposites is as follows. After MWCNTs are immersed into a dopamine alkaline solution, the dopamine monomer can be adsorbed on the MWCNTs via the $\pi-\pi$ stacking interaction between the aromatic dopamine and the graphitic framework (i.e., sp^2-hybridized carbons) of MWCNTs [36]. Then, alkaline solution can trigger the oxidative polymerization of dopamine, resulting in the MWCNTs coated with PDA layer [36].

As the as-prepared MWCNT-PDA composites are positively charged in acidic solution due to protonated amine groups of PDA [30], an electrostatic interaction occurs making $Fe(CN)_6^{3-}$ anions adhere to the composites after $Fe(CN)_6^{3-}$ acidic solution is added. The added Fe^{3+} subsequently coordinates with $Fe(CN)_6^{3-}$ on the surface of MWCNT-PDA composites, resulting in an $Fe^{III}-Fe^{III}(CN)_6^{3-}$ complex [26,37]. Electron transfer from MWCNT-PDA composites to the absorbed $Fe^{III}-Fe^{III}(CN)_6^{3-}$ complex can bring about the formation of PB nanostructure [24,27,37].

The spontaneous formation of PB on the surface of MWCNT-PDA can be explained by the different reduction potential between MWCNTs and the $Fe^{III}-Fe^{III}(CN)_6^{3-}$ complex [24,27,37]. The $Fe^{III}-Fe^{III}(CN)_6^{3-}$ complex is a very strong oxidant that has a high open circuit potential (about +1.22 V versus standard hydrogen electrode, SHE) in acidic media [37]. The Fermi level of SWNTs is approximately +0.5 V versus SHE [24]. Therefore, electrons spontaneously move from SWNTs to $Fe^{III}-Fe^{III}(CN)_6^{3-}$ complex.

Similar to that, a direct redox reaction between MWCNT-PDA composites and $Fe^{III}-Fe^{III}(CN)_6^{3-}$ complex can produce MWCNT-PDA-PB composites. In addition, the weak reducibility of PDA was also utilized to reduce the adsorbed $Fe^{III}-Fe^{III}(CN)_6^{3-}$ complex into PB NPs immobilized on the MWCNT-PDA surfaces [31,38]. Therefore, PB NPs are successfully produced on the surface of the MWCNT-PDA in a short time span.

3.2. Voltammetric behaviors of H_2O_2 at MWCNT-PDA-PB/GCE

Cyclic voltammetry was used in investigating the electrochemical behaviors of the MWCNT-PDA-PB nanocomposites modified GCE (MWCNT-PDA-PB/GCE). Figure 3A shows the cyclic voltammograms (CVs) of bare GCE, MWCNT-PDA/GCE, and MWCNT-PDA-PB/GCE in N_2 saturated 0.1 M KCl (pH 2.7) aqueous solution at a scan rate of 50 mV s^{-1}. One reversible pair of redox peaks is observed for MWCNT-PDA-PB/GCE in the potential between 0.2 and 0.5 V (Fig. 3A(c)) while no redox peaks were recorded for bare GCE (Fig. 3A(a)) and MWCNT-PDA/GCE (Fig. 3A(b)). According to previous studies [39,40], this redox pair was ascribed to the inter-conversion between Prussian blue (PB) and Prussian white (PW, reduction state of PB). After adding 5 mM H_2O_2, it was observed that the reduction peak increased greatly while the oxidation peak decreased slightly in MWCNT-PDA-PB/GCE (Fig. 3B(c)), indicating a typical electrocatalytic effect of PB toward H_2O_2 existed in the modified GCE.

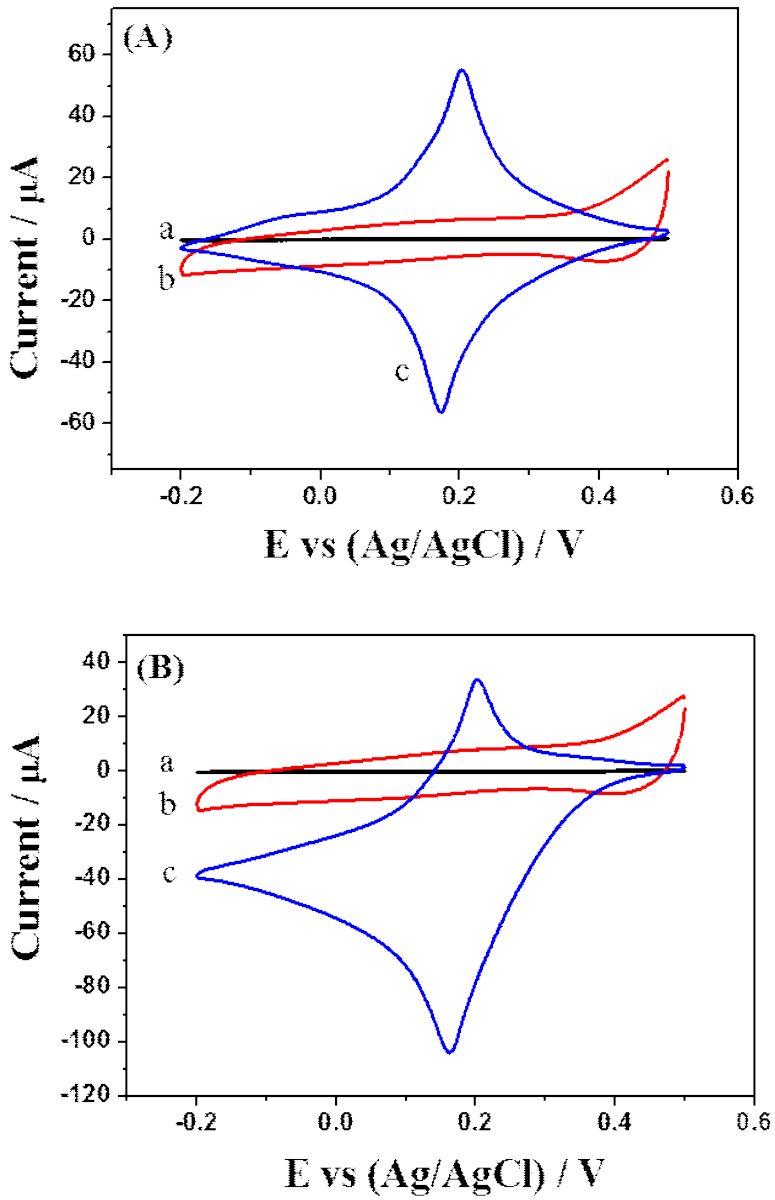

Figure 3. CVs of (a) bare GCE, (b) MWCNT-PDA/GCE, (c) MWCNT-PDA-PB/GCE in the absence (A) and presence of 5 mM H_2O_2 (B) from –0.2 to 0.5 V in N_2–saturated 0.1 M KCl solution (pH 2.7) at scan rate of 50 mV s^{-1}.

This electrocatalytic reaction between PB and H_2O_2 can be explained as follows [39]:

$$KFe^{III}[Fe^{II}(CN)_6]\ (PB) + K^+ + e^- \rightarrow K_2Fe^{II}[Fe^{II}(CN)_6]\ (PW) \quad (1)$$

$$2K_2Fe^{II}[Fe^{II}(CN)_6]\ (PW) + H_2O_2 + 2H^+ \rightarrow 2KFe^{III}[Fe^{II}(CN)_6]\ (PB) + 2H_2O + 2K^+ \quad (2)$$

In this cyclic mechanism, PB is first reduced to PW (Eq. (1)), which regenerates into PB, reducing the H_2O_2 (Eq. (2)) in the process. Therefore, the large cathodic current of H_2O_2 is observed at the redox potential of PB.

The cyclic voltammograms of MWCNT-PDA-PB/GCE in N_2-saturated 0.1 M KCl (pH 2.7) with different concentrations of H_2O_2 are shown in Fig. 4. The reduction peak current was increased in proportion to the H_2O_2 concentration, showing a linear relationship between them (inset in Fig. 4).

The electrochemical performances of the as-prepared nanocomposites was investigated at different scan rates. Figure 5 shows the effect of scan rate on the electrocatalytic H_2O_2 cathodic current in the range between 10 and 200 mV s^{-1}. The cathodic peak current are linear proportional to the square root of the scan rate (inset in Fig. 5), indicating that the electron transfer reaction is a diffusion-controlled process.

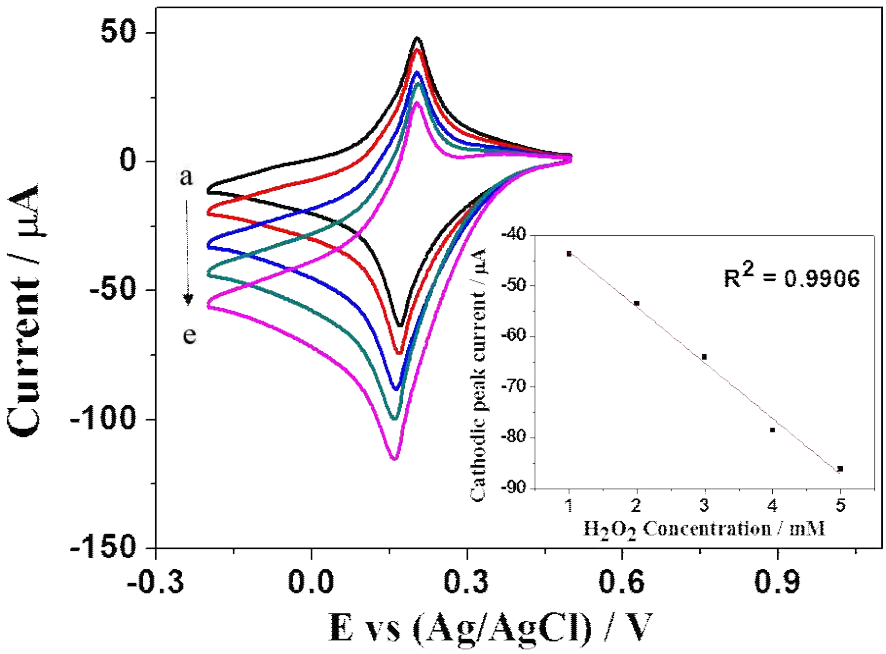

Figure 4. CVs of MWCNT-PDA-PB/GCE in N_2–saturated 0.1 M KCl aqueous solution (pH 2.7) in the presence of H_2O_2 with different concentrations (from a to e: 1, 2, 3, 4, and 5 mM) at a scan rate of 50 mV s^{-1}. Inset: plot of cathodic peak current versus H_2O_2 concentration.

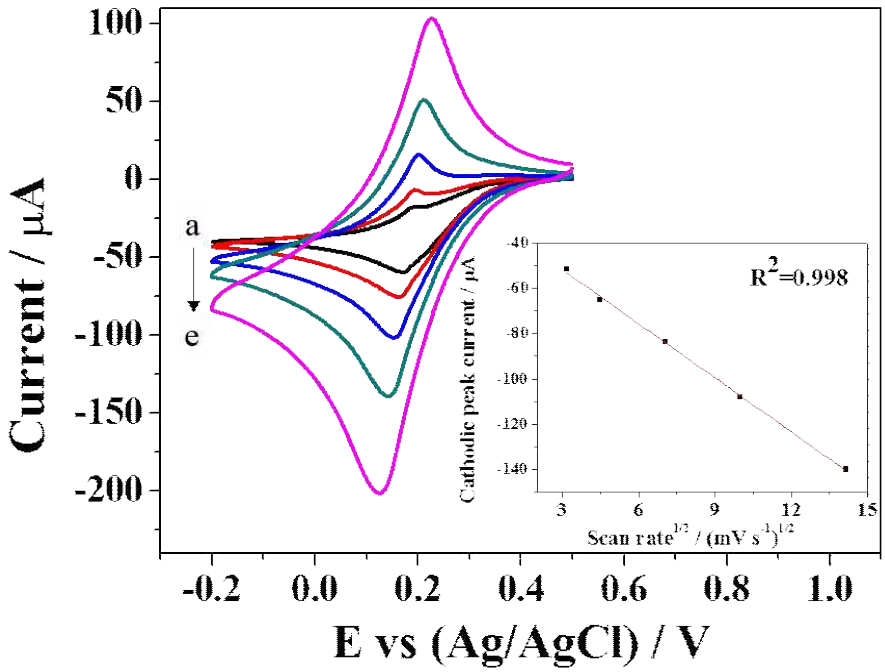

Figure 5. CVs of MWCNT-PDA-PB/GCE in N_2–saturated 0.1 M KCl aqueous solution (pH 2.7) in the presence of 5 mM H_2O_2 at different scan rates (from a to e: 10, 20, 50, 100, and 200 mV s^{-1}). Inset: plot of cathodic peak current versus scan rate.

3.3. Amperometric response of H_2O_2 at MWCNT-PDA-PB/GCE

The amperometric response of a GCE modified with MWCNT -PDA-PB at +0.1 V (vs. Ag/AgCl) in a solution containing 0.1M KCl (pH 2.7) is shown in Fig. 6A. The reduction current response was quickly enhanced as more H_2O_2 was added. The time required to reach the 95% steady-state response was less than 2 s. The rapid amperometric response is ascribed to the integration of PB and MWCNTs. The MWCNTs in the composites improve the electronic and potassium ionic transport capacity of the composites, resulting in a considerable enhancement of PB's electrocatalytic activity toward hydrogen peroxide reduction [41－43]. Figure 6B shows the calibration curve of reduction peak current versus concentration of H_2O_2. The linear range of the H_2O_2 detection was observed from 1 μM to 1.84 mM with a correlation coefficient of 0.9997, and the detection limit was about 0.039 μM with signal-to-noise ratio of 3. Corresponding sensitivity was estimated to be 351.2 μA mM^{-1} cm^{-2}, which was much higher than that obtained from MWCNT/PB/GCE (153.7 μA mM^{-1} cm^{-2}) [27] and PB NPs/Nafion/GCE (138.6 μA mM^{-1} cm^{-2}) [44]. The electrochemical characteristics of some CNT-PB based electrodes for the determining hydrogen peroxide are listed in Table 1. Our newly modified electrode shows improved sensitivity and detection limit in comparison to those of other reported electrodes.

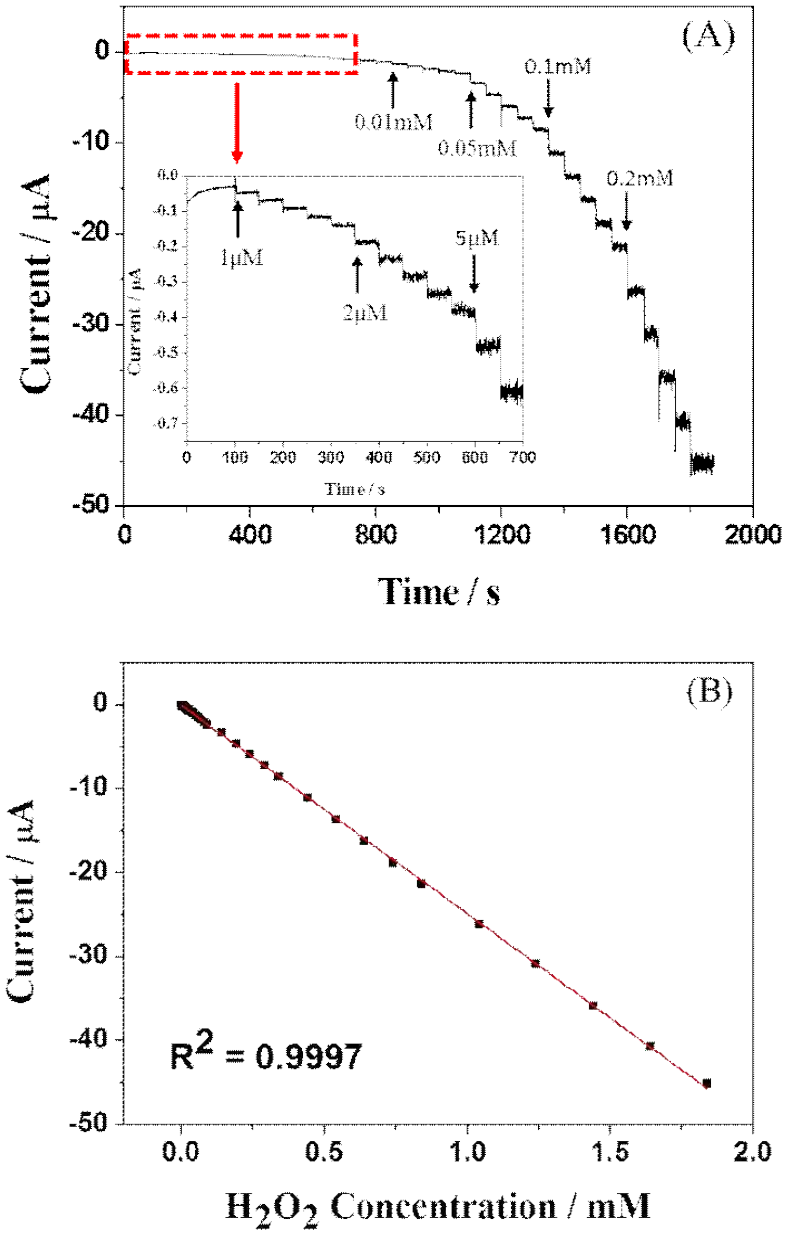

Figure 6. (A) Amperometric response of MWCNT-PDA-PB/GCE to successive injection of H_2O_2 in N_2–saturated 0.1 M KCl aqueous solution (pH 2.7) under stirring. Applied potential: 0.1 V. (B) Calibration curve of the reduction peak current versus concentration of H_2O_2.

Table 1. Electrochemical characteristics of various CNT-PB based electrodes designed for the determining of hydrogen peroxide.

Electrode	Linear range (mM)	Sensitivity ($\mu A\ mM^{-1}\ cm^{-2}$)	Limit of detection (μM)	Applied Potential (V)	References
PB-SWNTs/GCE	0.5 – 27.5	9.1	0.01	–0.1	[24]
MWCNT/PB/GCE	0.01 – 0.4	153.7	0.567	0	[27]
MWCNT/PPy/PB/GCE	410^{-3}– 0.517	345	0.08	–0.3	[28]
PBNPs/Nafion/GCE	2.110^{-3}– 0.14	138.6	1	–0.05	[44]
$[PB@Pt/PCNTs]_2$/GCE	2.510^{-4}– 1.5	850	0.15	0.1	[45]
MWNTs/PB/PG	10^{-3}–5	2400	1	–0.05	[46]
PB-MWCNT/Au	10^{-3}– 5	856	0.023	0.1	[47]
MWCNT/PVP/PB/Au	Nr	1300	0.025	0.1	[48]
MWCNT-PDA-PB/GCE	**10^{-3}–1.84**	**351.2**	**0.039**	**0.1**	**This work**

3.4. Selectivity, reproducibility, and stability

One of the most important challenge in the detection of hydrogen peroxide is to decrease the noise current generated by several reductants. Shown in Fig. 7 are amperometric responses of the modified electrode to the consecutive injections of hydrogen peroxide and typical electroactive species including ascorbic acid (AA), citric acid (CA), and L-cysteine (L-Cys) (0.1 mM, each). The influence of interfering species tested on the hydrogen peroxide was negligible, demonstrating a high selectivity of the proposed biosensor.

The novel biosensor displayed good reproducibility. Measurements of current response to 1 mM H_2O_2 for five different electrodes prepared under same conditions revealed a relative standard deviation (RSD) of 7.2%. The stability of the sensor was also investigated by measuring the response with 1 mM H_2O_2. After 50 scanning cycles, only 3.7% of the signal was lost, and after 100 scanning cycles, the loss of signal reached only 7.6%. The current response for 1 mM H_2O_2 kept 95.97% of the original value after 30 days when exposed to air at ambient conditions, indicating good stability.

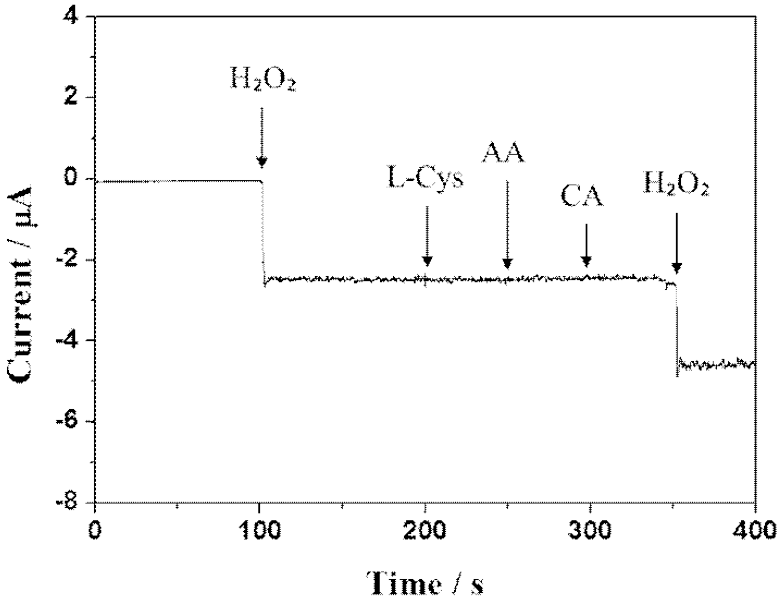

Figure 7. Amperometric response of MWCNT-PDA-PB/GCE on successive injection of H_2O_2, L-cysteine (L-Cys), ascorbic acid (AA), citric acid (CA) (0.1 mM, each) in N_2–saturated 0.1 M KCl (pH 2.7) under stirring. The working potential was +0.1 V.

4. Conclusions

This study has demonstrated that MWCNTs are easily functionalized by PDA without damaging the electronic structure and PB NPs can be uniformly and strongly adsorbed on the surface of MWCNTs using PDA. The PDA layer not only improved dispersion of MWCNTs in water, but also assisted the formation and immobilization of PB NPs on the surface of MWCNTs. The MWCNT-PDA-PB modified electrode displayed good electrocatalytic activity toward H_2O_2. Moreover, it exhibited a high sensitivity, low detection limit, and good stability compared with other MWCNT-PB based electrodes. Therefore, it is expected that this new method using PDA could be effective for the production of other carbon material-inorganic nanoparticle composites.

5. References

[1] S. Iijima, Helical microtubules of graphitic carbon, Nature. 354 (1991) 56–58.

[2] R.H. Baughman, A.A. Zakhidov, W.A. de Heer, Carbon nanotubes--the route toward applications, Science. 297 (2002) 787–92.

[3] F.G. Brunetti, M.A. Herrero, J.D.M. Muñoz, A. Díaz-Ortiz, J. Alfonsi, M. Meneghetti, et al., Microwave-induced multiple functionalization of carbon nanotubes, J. Am. Chem. Soc. 130 (2008) 8094–100.

[4] F.A. Lemasson, T. Strunk, P. Gerstel, F. Hennrich, S. Lebedkin, C. Barner-Kowollik, et al., Selective dispersion of single-walled carbon nanotubes with specific chiral indices by poly(N-decyl-2,7-carbazole), J. Am. Chem. Soc. 133 (2011) 652–5.

[5] Y.-P. Sun, K. Fu, Y. Lin, W. Huang, Functionalized carbon nanotubes: properties and applications, Acc. Chem. Res. 35 (2002) 1096–104.

[6] D. Tasis, N. Tagmatarchis, A. Bianco, M. Prato, Chemistry of carbon nanotubes, Chem. Rev. 106 (2006) 1105–36.

[7] C. Ménard-Moyon, F. Dumas, E. Doris, C. Mioskowski, Functionalization of single-wall carbon nanotubes by tandem high-pressure/Cr(CO)6 activation of Diels-Alder cycloaddition, J.

Am. Chem. Soc. 128 (2006) 14764–5.

[8] E. Mickelson, C. Huffman, Fluorination of single-wall carbon nanotubes, Chem. Phys. Lett. 296 (1998) 188–194.

[9] M.S. Strano, C. a Dyke, M.L. Usrey, P.W. Barone, M.J. Allen, H. Shan, et al., Electronic structure control of single-walled carbon nanotube functionalization, Science. 301 (2003) 1519–22.

[10] A. Star, D.W. Steuerman, J.R. Heath, J.F. Stoddart, Starched carbon nanotubes, Angew. Chem. Int. Ed. Engl. 41 (2002) 2508–12.

[11] J.K. Sprafke, S.D. Stranks, J.H. Warner, R.J. Nicholas, H.L. Anderson, Noncovalent binding of carbon nanotubes by porphyrin oligomers, Angew. Chem. Int. Ed. Engl. 50 (2011) 2313–6.

[12] A. Star, J.F. Stoddart, Dispersion and Solubilization of Single-Walled Carbon Nanotubes with a Hyperbranched Polymer, Macromolecules. 35 (2002) 7516–7520.

[13] F.J. Gómez, R.J. Chen, D. Wang, R.M. Waymouth, H. Dai, Ring opening metathesis polymerization on non-covalently functionalized single-walled carbon nanotubes, Chem. Commun. (2003) 190–191.

[14] H. Lee, S.M. Dellatore, W.M. Miller, P.B. Messersmith, Mussel-inspired surface chemistry for multifunctional coatings, Science. 318 (2007) 426–30.

[15] B. Fei, B. Qian, Z. Yang, R. Wang, W.C. Liu, C.L. Mak, et

al., Coating carbon nanotubes by spontaneous oxidative polymerization of dopamine, Carbon N. Y. 46 (2008) 1795–1797.

[16] K.-J. Huang, L. Wang, H.-B. Wang, T. Gan, Y.-Y. Wu, J. Li, et al., Electrochemical biosensor based on silver nanoparticles-polydopamine-graphene nanocomposite for sensitive determination of adenine and guanine., Talanta. 114 (2013) 43–8.

[17] X.-C. Liu, G.-C. Wang, R.-P. Liang, L. Shi, J.-D. Qiu, Environment-friendly facile synthesis of Pt nanoparticles supported on polydopamine modified carbon materials, J. Mater. Chem. A. 1 (2013) 3945.

[18] C. Ruan, W. Shi, H. Jiang, Y. Sun, X. Liu, X. Zhang, et al., One-pot preparation of glucose biosensor based on polydopamine–graphene composite film modified enzyme electrode, Sensors Actuators B Chem. 177 (2013) 826–832.

[19] J. Tian, S.-Y. Deng, D.-L. Li, D. Shan, W. He, X.-J. Zhang, et al., Bioinspired polydopamine as the scaffold for the active AuNPs anchoring and the chemical simultaneously reduced graphene oxide: characterization and the enhanced biosensing application., Biosens. Bioelectron. 49 (2013) 466–71.

[20] Y. Wang, L. Liu, M. Li, S. Xu, F. Gao, Multifunctional carbon nanotubes for direct electrochemistry of glucose oxidase and glucose bioassay., Biosens. Bioelectron. 30 (2011) 107–11.

[21] S. Chen, R. Yuan, Y. Chai, F. Hu, Electrochemical sensing of hydrogen peroxide using metal nanoparticles: a review,

Microchim. Acta. 180 (2012) 15–32.

[22] N. a Sitnikova, A. V Borisova, M. a Komkova, A. a Karyakin, Superstable advanced hydrogen peroxide transducer based on transition metal hexacyanoferrates, Anal. Chem. 83 (2011) 2359–63.

[23] A. a. Karyakin, E.E. Karyakina, Prussian Blue-based `artificial peroxidase' as a transducer for hydrogen peroxide detection. Application to biosensors, Sensors Actuators B Chem. 57 (1999) 268–273.

[24] W. Zhang, L. Wang, N. Zhang, G. Wang, B. Fang, Functionalization of Single-Walled Carbon Nanotubes with Cubic Prussian Blue and Its Application for Amperometric Sensing, Electroanalysis. 21 (2009) 2325–2330.

[25] H.C. Choi, M. Shim, S. Bangsaruntip, H. Dai, Spontaneous Reduction of Metal Ions on the Sidewalls of Carbon Nanotubes, J. Am. Chem. Soc. 124 (2002) 9058–9059.

[26] X.-W. Liu, Z.-J. Yao, Y.-F. Wang, X.-W. Wei, Graphene oxide sheet-prussian blue nanocomposites: green synthesis and their extraordinary electrochemical properties, Colloids Surf. B. Biointerfaces. 81 (2010) 508–12.

[27] J. Zhai, Y. Zhai, D. Wen, S. Dong, Prussian Blue/Multiwalled Carbon Nanotube Hybrids: Synthesis, Assembly and Electrochemical Behavior, Electroanalysis. 21 (2009) 2207–2212.

[28] E. Jin, X. Bian, X. Lu, C. Wang, Fabrication of multiwalled

carbon nanotubes/polypyrrole/Prussian blue ternary composite nanofibers and their application for enzymeless hydrogen peroxide detection, J. Mater. Sci. 47 (2012) 4326–4331.

[29] M. Lin, H. Huang, Y. Liu, C. Liang, S. Fei, X. Chen, et al., High loading of uniformly dispersed Pt nanoparticles on polydopamine coated carbon nanotubes and its application in simultaneous determination of dopamine and uric acid, Nanotechnology. 24 (2013) 065501.

[30] H. Hu, B. Yu, Q. Ye, Y. Gu, F. Zhou, Modification of carbon nanotubes with a nanothin polydopamine layer and polydimethylamino-ethyl methacrylate brushes, Carbon N. Y. 48 (2010) 2347–2353.

[31] Y. Wang, L. Liu, M. Li, S. Xu, F. Gao, Multifunctional carbon nanotubes for direct electrochemistry of glucose oxidase and glucose bioassay, Biosens. Bioelectron. 30 (2011) 107–11.

[32] E. Reguera, The existence of ferrous ferricyanide, Transit. Met. Chem. 24 (1999) 648–654.

[33] Y. Jiang, Y. Lu, L. Zhang, L. Liu, Y. Dai, W. Wang, Preparation and characterization of silver nanoparticles immobilized on multi-walled carbon nanotubes by poly(dopamine) functionalization, J. Nanoparticle Res. 14 (2012) 938.

[34] X. Wu, M. Cao, C. Hu, X. He, Sonochemical Synthesis of Prussian Blue Nanocubes from a Single-Source Precursor, Cryst. Growth Des. 6 (2006) 26–28.

[35] B.D. Cullity, Elements of X-ray Diffraction, Addison-Wesley Publishing Company, 1978.

[36] C. Shi, C. Deng, X. Zhang, P. Yang, Synthesis of highly water-dispersible polydopamine-modified multiwalled carbon nanotubes for matrix-assisted laser desorption/ionization mass spectrometry analysis., ACS Appl. Mater. Interfaces. 5 (2013) 7770–6.

[37] L. Wang, Y. Ye, H. Zhu, Y. Song, S. He, F. Xu, et al., Controllable growth of Prussian blue nanostructures on carboxylic group-functionalized carbon nanofibers and its application for glucose biosensing, Nanotechnology. 23 (2012) 455502.

[38] W. Ye, X. Shi, J. Su, Y. Chen, J. Fu, X. Zhao, et al., One-step reduction and functionalization protocol to synthesize polydopamine wrapping Ag/graphene hybrid for efficient oxidation of hydroquinone to benzoquinone, Appl. Catal. B Environ. 160-161 (2014) 400–407.

[39] A. Malinauskas, Electrocatalytic reactions of hydrogen peroxide at carbon paste electrodes modified by some metal hexacyanoferrates, Sensors Actuators B Chem. 46 (1998) 236–241.

[40] A. a. Karyakin, Prussian Blue and Its Analogues: Electrochemistry and Analytical Applications, Electroanalysis. 13 (2001) 813–819.

[41] J. Li, J.-D. Qiu, J.-J. Xu, H.-Y. Chen, X.-H. Xia, The Synergistic Effect of Prussian-Blue-Grafted Carbon

Nanotube/Poly(4-vinylpyridine) Composites for Amperometric Sensing, Adv. Funct. Mater. 17 (2007) 1574–1580.

[42] M. Zhang, W. Gorski, Electrochemical sensing based on redox mediation at carbon nanotubes., Anal. Chem. 77 (2005) 3960–5.

[43] M. Zhang, W. Gorski, Electrochemical sensing platform based on the carbon nanotubes/redox mediators-biopolymer system, J. Am. Chem. Soc. 127 (2005) 2058–9.

[44] B. Haghighi, H. Hamidi, L. Gorton, Electrochemical behavior and application of Prussian blue nanoparticle modified graphite electrode, Sensors Actuators B Chem. 147 (2010) 270–276.

[45] J. Zhang, J. Li, F. Yang, B. Zhang, X. Yang, Preparation of Prussian blue@Pt nanoparticles/carbon nanotubes composite material for efficient determination of H2O2, Sensors Actuators B Chem. 143 (2009) 373–380.

[46] Z. Li, J. Chen, W. Li, K. Chen, L. Nie, S. Yao, Improved electrochemical properties of prussian blue by multi-walled carbon nanotubes, J. Electroanal. Chem. 603 (2007) 59–66.

[47] D. Du, M. Wang, Y. Qin, Y. Lin, One-step electrochemical deposition of Prussian Blue–multiwalled carbon nanotube nanocomposite thin-film: preparation, characterization and evaluation for H2O2 sensing, J. Mater. Chem. 20 (2010) 1532.

[48] J. Li, J.-D. Qiu, J.-J. Xu, H.-Y. Chen, X.-H. Xia, The Synergistic Effect of Prussian-Blue-Grafted Carbon Nanotube/Poly(4-vinylpyridine) Composites for Amperometric Sensing, Adv. Funct. Mater. 17 (2007) 1574–1580.

국문 요약

탄소나노튜브-폴리도파민-프러시안 블루 나노복합물의 합성과 과산화수소의 검출 연구

본 연구에서는 다중벽 탄소나노튜브 (Multi-walled carbon nanotubes, MWCNTs)-폴리도파민 (Polydopamine, PDA)-프러시안 블루 (Prussian blue, PB) 나노복합물을 합성하는 간단한 방법을 제시했다. 상온에서 도파민 수용액에 분산시킨 다중벽 탄소나노튜브는 폴리도파민에 의해 간단히 코팅되었다. 여기에 페리사이안화칼륨($K_3Fe(CN)_6$) 용액과 염화철(Ⅲ)($FeCl_3$) 용액을 넣고 1 시간동안 부드럽게 교반하면 프러시안 블루 나노입자가 다중벽 탄소나노튜브-폴리도파민 복합물 위에 형성된다. 폴리도파민 층은 다중벽 탄소나노튜브를 물에 잘 분산되게 할 뿐 아니라, 다중벽 탄소나노튜브 표면에서 프러시안 블루 나노입자가 형성되고 고정되는 것을 돕는다.

만들어진 다중벽 탄소나노튜브-폴리도파민-프러시안 블루 나노복합물의 구조적 특성과 화학 조성은 투과전자현미경 (Transmission electron microscopy, TEM), X-선 회절법 (X-ray diffraction, XRD), 푸리에 변환 적외분광법 (Fourier transform infrared spectroscopy, FT-IR) 등을 이용해 분석했다. 이렇게 만들어진 나노복합물 분산액을 유리탄소전극 (Glassy carbon electrode, GCE)에 떨어뜨려 말리는 방법으

로 다중벽 탄소나노튜브-폴리도파민-프러시안 블루로 수정된 유리탄소 전극을 제작했다.

다중벽 탄소나노튜브-폴리도파민-프러시안 블루로 수정된 유리탄소 전극의 전기화학적 활동을 알아보고자 순환전압전류법 (Cyclic voltammetry, CV), 시간전류법 (Amperometry) 등의 분석방법을 사용하였다. 수정된 전극은 과산화수소의 환원에 대해 우수한 전기화학적 촉매 반응을 나타냈다. 이 센서는 과산화수소 측정 실험에서 선형 구간 0.001-1.84 mM, 감도 351.2 μA mM^{-1} cm^{-2} , 검출한계 0.039 μM (S/N=3) 의 값을 나타냈는데, 이것은 기존의 발표된 탄소나노튜브-프러시안 블루 기반 전극들의 전극 특성에 비해 우수한 결과이다.

본 연구에서는 폴리도파민의 다기능적 성질 (자가중합, 흡착성, 친수성)을 활용한 탄소나노튜브 표면 개질 방법과 탄소나노튜브와 무기나노입자의 결합 방법을 제안했다. 이 방법들은 앞으로 다양한 분야에 활용될 수 있을 것으로 생각한다.

주요어: 다중벽 탄소나노튜브, 폴리도파민, 프러시안 블루, 과산화수소, 시간전류법.

***Student Number* : 2013-21424**